

Chapter 1

EMPIRICAL TESTS FOR EVALUATION OF MULTIRATE FILTER BANK PARAMETERS

Carl Taswell
Computational Toolsmiths
P.O. Box 18925
Stanford, CA 94309-8925
ctaswell@toolsmiths.com

Abstract Empirical tests have been developed for evaluating the numerical properties of multirate M -band filter banks represented as $N \times M$ matrices of filter coefficients. Each test returns a numerically observed estimate of a $1 \times M$ vector parameter in which the m^{th} element corresponds to the m^{th} filter band. These vector valued parameters can be readily converted to scalar valued parameters for comparison of filter bank performance or optimization of filter bank design. However, they are intended primarily for the characterization and verification of filter banks. By characterizing the numerical performance of analytic or algorithmic designs, these tests facilitate the experimental verification of theoretical specifications.

Tests are introduced, defined, and demonstrated for M -shift biorthogonality and orthogonality errors, M -band reconstruction error and delay, frequency domain selectivity, time frequency uncertainty, time domain regularity and moments, and vanishing moment numbers. These tests constitute the verification component of the first stage of the hierarchical three stage framework (with filter bank coefficients, single-level convolutions, and multi-level transforms) for specification and verification of the reproducibility of wavelet transform algorithms.

Filter banks tested as examples included a variety of real and complex orthogonal, biorthogonal, and nonorthogonal M -band systems with $M \geq 2$. Coefficients for these filter banks were either generated by computational algorithms or obtained from published tables. Analysis of these examples from the published literature revealed previously undetected errors of three different kinds which have been called transmission, implementation, and interpretation errors. The detection of these mistakes demonstrates the importance of the evaluation methodology in revealing past and preventing future discrepancies between observed and

expected results, and thus, in insuring the validity and reproducibility of results and conclusions based on those results.

1. Introduction

Multirate M -band filter banks play many important roles in diverse engineering systems, not least of which is their use as the key engine of iteration in wavelet transform algorithms. Their critical importance in these algorithms warrants unambiguous specification and verification in any effort to insure the scientific and engineering reproducibility of results obtained with them. This reproducibility has been defined [11, 15] as the requirement that the specified algorithm yield the same results for the same data regardless of implementation in any programming language on any computing machine. Moreover, a methodology to evaluate reproducibility in this context has been designed [11, 15] as a three stage framework with hierarchical and polymorphic structures and operators. Filter bank coefficients, single-level convolutions, and multi-level transforms constitute the three stages of this framework. Each stage requires both a specification and a verification component. Use of this evaluation methodology facilitates the detection of errors in filter banks and transform algorithms as well as other discrepancies between theoretically expected and experimentally observed results.

As described in [11, 15], specification of the filter bank coefficients necessitates either tabulation of the coefficients or definition of the computational algorithm that generates the coefficients, while verification of the filter bank involves characterization of the filter bank's properties with numerical estimates of parameters such as the reconstruction error, frequency domain selectivity, time domain regularity, *et c.* Most importantly, if a filter bank is designed to possess certain characteristics in the specification, then experimentally observed results for those theoretically expected characteristics must be evaluated *independently* in the verification. However, the details of this evaluation methodology were not elaborated in [11, 15]. Therefore, in this report, detailed computational algorithms are introduced in Section 2 for a comprehensive suite of novel tests for filter bank evaluation including the M -shift biorthogonality and orthogonality errors, M -band reconstruction error and delay, frequency domain selectivity, time frequency uncertainty, time domain regularity, time domain centers and moments, and vanishing moment numbers, each of which is valid for all M -bands of the M -band filter banks.

The evaluation tests are then demonstrated in Section 3 on a diverse variety of M -band wavelet filter banks. Using the names and acronyms

summarized here, these filters include the Daubechies Real Biorthogonal Balanced Regular (DRBBR) and Complex Orthogonal Most Symmetric (DCOMS) [12, 16], Rioul Real Orthogonal Most Selective (RROMS) [8], Heller Real Orthogonal M -band K -regular (HROMK) [3], Sherlock Real Orthogonal 2-band 1-regular [9] parameterized with Random Angles (SRORA), Hermite Real Nonorthogonal Symmetric Binomial (HRNSB) [2], and a wide assortment of filter banks available from Nayebi *et al.* [5]. The filter banks chosen as test examples were selected to represent a variety of different classes with contrasting features. In addition, representative examples were selected for both kinds of specification, *i.e.*, filter coefficients generated by computational algorithms and filter coefficients listed in published tables. Finally, the evaluation methodology and those test examples observed to incur errors are discussed in Section 4 with respect to the importance of using the methodology to 1) detect errors in filter banks and their generating algorithms and 2) reveal significant discrepancies between theoretically expected and experimentally observed results. Some of the methods presented here have previously appeared in the conference paper [14]. All of them have been used throughout the development of the systematized collection of Daubechies wavelets by Taswell [17, 19].

2. Methods

2.1. Notation and Conventions for Filter Banks

Consider an arbitrary M -band analysis and synthesis system with uniform downsampling and upsampling rate R . This system has M analysis filters $\mathbf{a}_m \equiv a_m[n]$, M downsamplers and upsamplers operating at rate R , and M synthesis filters $\mathbf{s}_m \equiv s_m[n]$ where $m = 0, 1, \dots, M-1$ is the band index and $n = 0, 1, \dots, N-1$ is the time index. Here $N = BR$ is an integer multiple $B = \lceil (\max_m N_m)/R \rceil$ of R determined with the maximum of the minimum support lengths N_m of \mathbf{a}_m . The first nonzero coefficient of each \mathbf{a}_m is indexed at time step $n = 0$ and any filter with length $N_m < N$ is padded with trailing zeros. The first nonzero coefficient of each \mathbf{s}_m is indexed at a time step $n \geq 0$ and padded with either leading or trailing zeros or both as long as the total length with padding is constrained to N .

All filters in the system can then be represented as the $N \times M$ matrices $\mathbf{A} \equiv [a_{nm}]$ and $\mathbf{S} \equiv [s_{nm}]$ with time index n increasing down the rows and band index m increasing across the columns. This convention permits columnwise tabulation and display of the coefficients and facilitates convenient columnwise data analysis for the band filters in each of the columns. Individual filters in the filter banks can be readily

characterized by computing various measures, such as norms and statistical moments, of each column of coefficients in the matrices. Thus, for each type of parameter characterizing a given filter bank, there is a corresponding $1 \times M$ vector of parameter estimates for the M columns of the filter bank.

To fix the normalization of a filter bank, assume that an $N \times M$ filter bank \mathbf{H} has been given with a lowpass filter \mathbf{h}_0 that has a nonzero coefficient sum $\sum_n h_0[n] \neq 0$. Then given a normalization constant η for the desired \mathbf{F} to be obtained from the given \mathbf{H} , compute the η -normalized \mathbf{F} with

$$\mathbf{f}_m = \left(\eta / \sum_{n=0}^{N-1} h_0[n] \right) \mathbf{h}_m \quad (1.1)$$

for $m = 0, 1, \dots, M - 1$ which yields the desired constant $\eta = \sum_n f_0[n]$ as coefficient sum for the lowpass filter \mathbf{f}_0 . For an alternate type of normalization, consider the uniform unit band energy normalization

$$\mathbf{f}_m = \left(\sum_{n=0}^{N-1} |h_m[n]|^2 \right)^{-1/2} \mathbf{h}_m \quad (1.2)$$

which is computed independently for each band $m = 0, 1, \dots, M - 1$ and does not require a normalization constant.

2.2. Iteration of Multirate Filter Banks

The filter coefficients themselves constitute the discrete impulse responses for the FIR filters of the filter bank. Iterative interpolation with upscaling approximation yields estimates of the continuous impulse responses for the functions corresponding to the filters. In the following development of notation, the discussion begins with a 2-band wavelet system where \mathbf{f} and \mathbf{g} are used instead of \mathbf{f}_0 and \mathbf{f}_1 for the lowpass scalet and highpass wavelet filters, respectively. Then later for the M -band case, the notation will return to the more general expressions with \mathbf{f}_m .

For the iterates $\{f^{(j)}[n] | j = 0, 1, 2, \dots\}$ of the lowpass scalet filter $f[n]$ with length N and normalization $\eta = 2$, let $f^{(0)}[n] = f[n]$ be the initial discrete impulse response and let the recursion

$$f^{(j+1)}[n] = \sum_{k=0}^{N-1} f[k] f^{(j)}[n - 2k] \quad (1.3)$$

determine the sequential estimates $\mathbf{f}^{(j)}$ of the continuous impulse response approximating the corresponding scalet function

$$\phi(t) = \sum_{k=0}^{N-1} f[k]\phi(2t - k) \quad (1.4)$$

defined by an implicit two-scale equation relating ϕ to itself.

Analogously, for the iterates $\{g^{(j)}[n] | j = 0, 1, 2, \dots\}$ of the highpass wavelet filter $g[n]$, let $g^{(0)}[n] = g[n]$ be the initial discrete impulse response and let

$$g^{(j+1)}[n] = \sum_{k=0}^{N-1} g[k]f^{(j)}[n - 2k] \quad (1.5)$$

determine the sequential estimates $\mathbf{g}^{(j)}$ of the continuous impulse response approximating the corresponding wavelet function

$$\psi(t) = \sum_{k=0}^{N-1} g[k]\phi(2t - k) \quad (1.6)$$

defined by an explicit two-scale equation relating ψ to ϕ .

More generally, for an M -band filter bank \mathbf{F} with normalization $\eta = M$ and upsampling rate $R = M$, let $\mathbf{Y}^{(0)} = \mathbf{F}$ be the set of initial discrete impulses with matrix $\mathbf{Y} \equiv [y_{nm}]$ and column vectors $\mathbf{y}_m^{(0)} = \mathbf{f}_m$ for $m = 0, 1, \dots, M - 1$. Then let

$$y_m^{(j+1)}[n] = \sum_{k=0}^{N-1} f_0[k]y_m^{(j)}[n - Mk] \quad (1.7)$$

be the estimates of the continuous impulse responses approximating the corresponding scalet and wavelet functions

$$\left. \begin{array}{l} \phi(t) \\ \psi_m(t) \end{array} \right\} = \sum_{k=0}^{N-1} f_m[k]\phi(Mt - k) \text{ for } \left\{ \begin{array}{l} m = 0 \\ m = 1, \dots, M - 1 \end{array} \right. \quad (1.8)$$

defined by the M -scale equations relating ϕ or ψ_m to ϕ . After J iterations, obtain the approximations

$$\left. \begin{array}{l} \phi(t_n) \\ \psi_m(t_n) \end{array} \right\} \approx y_m^{(J)}[n] \text{ for } \left\{ \begin{array}{l} m = 0 \\ m = 1, \dots, M - 1 \end{array} \right. \quad (1.9)$$

with discrete samples indexed by n at continuous times $t_n = nM^{-J-1}$. For simplicity of notation in the remainder of the text, let ψ_0 denote ϕ .

2.3. Kronecker Delta Error $\text{kde}(\mathbf{f})$

In the following development of definitions and tests for various filter parameters, it will be convenient to base some of them on an underlying test of an arbitrary vector $\mathbf{f} \equiv f[n]$ for its approximation to a Kronecker delta vector. Let $\boldsymbol{\delta}_k \equiv \delta_k[n]$ denote the Kronecker delta vector with a single nonzero element $\delta_k[n] = 1$ at time index $n = k$. Then define the Kronecker delta delay d and error e with

$$d = \text{kdd}(\mathbf{f}) = \underset{n}{\operatorname{argmax}} |f[n]| \quad (1.10)$$

$$\begin{aligned} e = \text{kde}(\mathbf{f}) &= \operatorname{error}(\mathbf{f}, \boldsymbol{\delta}_d) \\ &= \max_n |f[n] - \delta_d[n]| \end{aligned} \quad (1.11)$$

where $\operatorname{error}(\cdot, \cdot)$ can be any appropriate error function such as an ℓ^p vector norm of the difference of the arguments, for example as shown here, the maximum absolute value error with the ℓ^∞ norm. Note that d indexes the time location expected for the Kronecker delta spike in \mathbf{f} .

2.4. M -Shift Biorthogonality Error $\text{mbe}(\mathbf{A}, \mathbf{S})$

Assume two filter vectors \mathbf{a} and \mathbf{s} of minimum support length N_a and N_s , respectively, each with first nonzero coefficient aligned to time index $n = 0$. Construct the $K \times M$ matrix $\mathbf{C} \equiv [c_{km}]$ from the M -shift m -delay convolutions $(\cdot *_m \cdot)$ of the two filter vectors \mathbf{a} and \mathbf{s} with resulting column vectors $\mathbf{c}_m = \mathbf{a} *_m \mathbf{s}$ defined by

$$c_m[k] = \sum_{n=0}^{N-1} a[n]s[m + kM + N - n] \quad (1.12)$$

for $m = 0, \dots, M - 1$ and $k = 0, \dots, K - 1$ where $N = \max(N_a, N_s)$ and $K = \lceil N/M \rceil$. Compute the Kronecker delta errors for the column vectors \mathbf{c}_m of the matrix \mathbf{C} . Then

$$e_m = \text{kde}(\mathbf{c}_m) = \text{kde}(\mathbf{a} *_m \mathbf{s}) \quad (1.13)$$

$$d = \text{mbd}(\mathbf{a}, \mathbf{s}) = \underset{m}{\operatorname{argmin}} e_m \quad (1.14)$$

$$e = \text{mbe}(\mathbf{a}, \mathbf{s}) = \min_m e_m \quad (1.15)$$

determines M -shift m -delay biorthogonality for the two filter vectors \mathbf{a} and \mathbf{s} with observed delay d and error e . Note that d represents the relative delay between the two vectors in the m -delay convolution $(\cdot *_m \cdot)$. This delay is distinct from the delay defined for the Kronecker delta spike in Section 2.3.

To determine the mutual biorthogonality of the filters in the $N \times M$ filter bank matrices \mathbf{A} and \mathbf{S} , define the $M \times M$ matrix $\mathbf{E} \equiv [e_{ij}]$ with

$$e_{ij} = \begin{cases} \text{mbe}(\mathbf{a}_i, \mathbf{s}_j) & \text{if } i = j \\ \min_m \text{error}(\mathbf{a}_i *_m \mathbf{s}_j, \mathbf{0}) & \text{if } i \neq j \end{cases} \quad (1.16)$$

where $\mathbf{0}$ is the zero vector. For consistency with the previous default type of error function used for the `mbe` and `kde` functions, the `error` function here should be taken as the maximum absolute value error. Then define the $1 \times M$ vector $\mathbf{e} \equiv [e_j]$ with

$$e_j = \max_i e_{ij} \quad (1.17)$$

as the error of biorthogonality for each band of the M -band filter banks. Summarizing for both a pair of filters as well as a pair of filter banks, denote the M -shift biorthogonality errors with

$$e = \text{mbe}(\mathbf{a}, \mathbf{s}) \quad (1.18)$$

$$\mathbf{e} = \text{mbe}(\mathbf{A}, \mathbf{S}). \quad (1.19)$$

The above definition of mutual M -shift biorthogonality for the band filter column vectors of the filter bank matrices \mathbf{A} and \mathbf{S} does not necessarily imply the biorthogonality of \mathbf{A} and \mathbf{S} as linear operator matrices.

2.5. M -Shift Orthogonality Error $\text{moe}(\mathbf{F})$

Given the above definitions for M -shift biorthogonality, then define M -shift orthogonality for a filter vector \mathbf{f} or filter bank matrix \mathbf{F} as the M -shift biorthogonality of the vector \mathbf{f} and its paraconjugate \mathbf{f}^P or of the matrix \mathbf{F} and its paraconjugate \mathbf{F}^P . Thus, define the M -shift orthogonality errors for \mathbf{f} and \mathbf{F} with

$$e = \text{moe}(\mathbf{f}) = \text{mbe}(\mathbf{f}, \mathbf{f}^P) \quad (1.20)$$

$$\mathbf{e} = \text{moe}(\mathbf{F}) = \text{mbe}(\mathbf{F}, \mathbf{F}^P). \quad (1.21)$$

Again, note that this definition of mutual M -shift orthogonality for the M column vectors of \mathbf{F} as a filter bank matrix does not necessarily imply the orthogonality of \mathbf{F} as a linear operator matrix.

2.6. M -Band Reconstruction Error $\text{mre}(\mathbf{A}, \mathbf{S})$

Two empirical tests for the M -band reconstruction error

$$\mathbf{e} = \text{mre}(\mathbf{A}, \mathbf{S}) \quad (1.22)$$

for the analysis synthesis filter bank system $\{\mathbf{A}, \mathbf{S}\}$ have been implemented as appropriate modifications of perfect reconstruction criteria

published elsewhere. Both tests are based on time domain conditions for exact reconstruction: the unique operator criterion of Rioul [7, pg.2595, eqn.21] for the downscaling and upscaling operators associated with \mathbf{A} and \mathbf{S} , and the time delayed block reconstruction criterion of Nayebi *et al.* [5, pg.1415, eqn.30] for the output blocks of size $M \times M$ when downsampling and upsampling rates $R = M$ for both \mathbf{A} and \mathbf{S} . Since the latter test proves to be more general as well as more convenient for the empirical determination of the M -band reconstruction delay

$$\mathbf{d} = \text{mrd}(\mathbf{A}, \mathbf{S}) \quad (1.23)$$

it was used for the numerical computation of the values \mathbf{e} and \mathbf{d} reported here for M -band filter banks. Note that $\max(\mathbf{d}) \in \mathbb{N}$ measures the delay in time samples for reconstruction of an impulse processed through the filter bank system. For a correctly implemented system, all empirical estimates $\{d_m \mid m = 0, \dots, M - 1\}$ should equal the expected delay Δ that has been designed for the filter bank. Finally, note that the original criterion described by Nayebi *et al.* [5] was intended for use in a design and optimization algorithm rather than for use in independent tests of reconstruction error and system delay. Thus, the essential extension implemented here is the modification of the original criterion for use in evaluating the errors and delays of each of the bands in the M -band filter bank.

2.7. Time Domain Moments $\text{tdm}(\mathbf{F})$

Given the $N \times M$ filter bank matrix \mathbf{F} with band filters \mathbf{f}_m , generate the estimates of $\psi_m(t_n)$ with $y_m^{(J)}[n]$ as explained in Section 2.2 leading to Equation 1.9. Then define the q^{th} power weighted discrete and continuous time domain centers

$$c_{mq} = \left\langle \left(\sum_{n=0}^{N-1} n |f_m[n]|^q \right) / \left(\sum_{n=0}^{N-1} |f_m[n]|^q \right) \right\rangle \quad (1.24)$$

$$\gamma_{mq} = \left(\int t |\psi_m(t)|^q dt \right) / \left(\int |\psi_m(t)|^q dt \right) \quad (1.25)$$

where the discrete center c_{mq} is integer, the continuous center γ_{mq} is real, and $\langle \cdot \rangle$ in this context denotes rounding to the nearest integer. Identifying $J = 0$ and $J > 0$ with the discrete and continuous centers respectively for the filters and functions, that is, identifying $\psi_m(t_n)$ with $y_m^{(J)}[n]$ for $J > 0$ and $f_m[n]$ with $y_m^{(J)}[n]$ for $J = 0$ as in Section 2.2, and then applying numerical integration for the case of the continuous functions (see examples below), compute the parameter estimates as the

outputs of the function

$$\text{tdc}(\mathbf{f}_m; J, q) = \begin{cases} c_{mq} & \text{if } J = 0 \\ \gamma_{mq} & \text{if } J > 0. \end{cases} \quad (1.26)$$

For $q = 1$ and $q = 2$, the weighted centers correspond to the centers of mass and energy, respectively. For $q = \infty$, it can be redefined to be the abscissa corresponding to the ordinate with peak magnitude.

With the weighted centers, define the p^{th} discrete and continuous time domain moments

$$k_{mpq} = \sum_{n=0}^{N-1} (n - c_{mq})^p f_m[n] \quad (1.27)$$

$$\kappa_{mpq} = \int (t - \gamma_{mq})^p \psi_m(t) dt \quad (1.28)$$

where both k_{mpq} and κ_{mpq} are real. Since $\psi_m(t_n) \approx y_{mn}^{(J)}$ at $t_n = nM^{-J-1}$, the continuous integral can be numerically approximated by a discrete sum

$$\int (t - \gamma_{mq})^p \psi_m(t) dt \approx M^{-J-1} \sum_n (t_n - \gamma_{mq})^p y_{mn}^{(J)} \quad (1.29)$$

or with a particular quadrature rule such as Simpson's rule or the trapezoidal rule. Again, identifying $J = 0$ and $J > 0$ with the discrete and continuous versions respectively, compute the estimates after J iterations as the outputs of the function

$$\text{tdm}(\mathbf{f}_m; J, p, q) = \begin{cases} k_{mpq} & \text{if } J = 0 \\ \kappa_{mpq} & \text{if } J > 0. \end{cases} \quad (1.30)$$

More explicitly, compute

$$\text{tdm}(\mathbf{f}_m; J, p, q) = \begin{cases} \sum_{n=0}^{N-1} (n - c_{mq})^p y_{mn}^{(J)} & \text{if } J = 0 \\ \text{numint}((t_n - \gamma_{mq})^p y_{mn}^{(J)}, M^{-J-1}) & \text{if } J > 0 \end{cases} \quad (1.31)$$

where the function `numint` for numerical integration accepts a vector first argument for the ordinate values to be integrated and a scalar second argument for the uniform increment of the abscissa values. By default, assume that the centers from $\text{tdc}(\mathbf{f}; J, q)$ and the moments from $\text{tdm}(\mathbf{f}; J, p, q)$ are determined with the same J and the same $q = 2$, and that the numerical integration is performed according to the trapezoidal quadrature rule. For convenience, summarize the notation with output

vector parameters for input matrix filter banks with

$$\boldsymbol{\gamma}_J \equiv [\gamma_{mJ}] = \text{tdc}(\mathbf{F}; J) \quad (1.32)$$

$$\boldsymbol{\kappa}_{Jp} \equiv [\kappa_{mJp}] = \text{tdm}(\mathbf{F}; J, p) \quad (1.33)$$

also suppressing both the default $q = 2$ and the notation for the distinctions between discrete and continuous centers c_m and γ_m and moments k_m and κ_m for $J = 0$ and $J > 0$.

2.8. Vanishing Moments Numbers $\text{vmn}(\mathbf{F})$

Now consider the numerically observed vanishing moments number for \mathbf{f}_m to be the integer ν_{mJ} obtained from the sequence of real $\{\kappa_{mJp} | p = 0, 1, \dots\}$ using an absolute zero criterion

$$\nu_{mJ} = \text{vmn}(\mathbf{f}_m; J, \epsilon_{\text{abs}}) = \min_{p|\chi=1} (p+1) \chi(|\kappa_{mJp}| > \epsilon_{\text{abs}}) \quad (1.34)$$

with tolerance $\epsilon_{\text{abs}} \approx 0$ such as $\epsilon_{\text{abs}} = 1 \times 10^{-4}$, or using a relative jump criterion

$$\nu_{mJ} = \text{vmn}(\mathbf{f}_m; J, \epsilon_{\text{rel}}) = \min_{p|\chi=1} (p+1) \chi(|\kappa_{m,J,p+1}/\kappa_{mJp}| > \epsilon_{\text{rel}}) \quad (1.35)$$

with tolerance $\epsilon_{\text{rel}} \gg 1$ such as $\epsilon_{\text{rel}} = 1 \times 10^4$, where $\chi(\cdot)$ is a Boolean logic indicator function returning the truth value $\chi \in \{0, 1\}$ for its expression argument.

For bandpass or highpass wavelet filters, all values of p such that $\chi = 1$ are examined. However, for lowpass scalet filters, all p such that $\chi = 1$ excluding $p = 0$ are examined as necessitated by the fact that the lowpass filter must have a nonvanishing zeroth moment. For the matrix \mathbf{F} , assume that \mathbf{f}_0 is a lowpass filter and test it with $p \geq 1$; assume that all other \mathbf{f}_m are bandpass or highpass filters and test them with $p \geq 0$. Denote the ϵ -tolerant vanishing moments numbers after J iterations of the filter bank \mathbf{F} as the $1 \times M$ vector

$$\boldsymbol{\nu}_J \equiv [\nu_{mJ}] = \text{vmn}(\mathbf{F}; J, \epsilon). \quad (1.36)$$

By default, assume for $\text{vmn}(\cdot; \cdot, \cdot)$ that $J = 2$ and $\epsilon = \epsilon_{\text{abs}}$ with the absolute zero criterion test for \mathbf{F} normalized to $\eta = R$ where the upsampling rate $R = M$ if $M > 1$ else $R = 2$ if $M = 1$. Again, note that the moments $\boldsymbol{\kappa}_{Jp}$ are real M -vectors for a given J and p while the numbers $\boldsymbol{\nu}_J$ are integer M -vectors for a given J . For examples demonstrating the distinction between estimating $\boldsymbol{\nu}_J$ with the absolute zero versus relative jump criteria, refer to Figures 2–4 of [14].

2.9. Time Domain Regularity $\text{tdr}(\mathbf{F})$

Various definitions and methods are available in the literature for estimating the regularity of a function. Here we discuss a previously unpublished method for estimating the time domain regularity, denoted $\text{tdr}(\mathbf{F})$, of a filter bank's estimated continuous time impulse responses $y_m^{(j)}[n]$ generated iteratively as explained in Section 2.2 from its discrete time impulse responses $f_m[n]$. This method was first used in Version 4.0a3 (12-Jan-1994) of the $\mathcal{W}\mathcal{A}\mathcal{V}\mathcal{B}\mathcal{X}$ Software Library [10] with a summary of the method reported in [14]. An iterative estimate of the time domain regularity can be evaluated by applying to Rioul's definition of Holder regularity for subdivision schemes [6] a general procedure for determining the convergence order of a sequence of functions.

Assume an arbitrary continuous time function $y(t)$ approximated at iterations j and time points $t_n = nh_j$ by $y^{(j)}[n]$ with error function $e^{(j)}[n] = y(t_n) - y^{(j)}[n]$ where t_n is real, n is integer, and $h_j > 0$ is real $h_j \rightarrow 0$ as $j \rightarrow \infty$. Let $e^{(j)}[n] = \mathcal{O}(h_j^q)$ as $h_j \rightarrow 0$ mean that there exist constants C and h_0 such that $|e^{(j)}[n]| \leq Ch_j^q$, $\forall n, \forall h_j \leq h_0$. We can think of the corresponding continuous $e(t)$ as an error function for which we desire ideally $e(t) \approx 0$, $\forall t$.

Now evaluate $e^{(j)}[n]$ for the sequence $\{h_j \mid j = 0, 1, 2, \dots\}$ where $h_0 > h_1 > h_2 > \dots > 0$. In particular, take $h_j = h_0/c^j$ for $j = 1, 2, \dots$ where c is another arbitrary constant $c > 1$, say $c = R$ appropriate for iterative sequences generated by upscaling with filters at rate $R = M$ from an M -band filter bank with $M \geq 2$. Define $e_j = \max_n |e^{(j)}[n]|$ so that $e_j \leq Ch_j^q$ and $e_{j+1} \leq Ch_{j+1}^q$. Then derive

$$\frac{e_j}{e_{j+1}} \approx \frac{Ch_j^q}{Ch_{j+1}^q} = \frac{(h_0/c^j)^q}{(h_0/c^{j+1})^q} = c^q \quad (1.37)$$

for which we can estimate

$$q_j = \frac{\log(e_j/e_{j+1})}{\log(c)} \quad (1.38)$$

with ideally $q = \lim_{j \rightarrow \infty} q_j$.

To account for convergence that is nonmonotonic or even oscillatory, we can use smoothers such as the median to define the estimate

$$\hat{q}_j = \text{med}\{q_i \mid i = j_0, j_0 + 1, \dots, j\} \quad (1.39)$$

as well as the lower and upper bounds

$$\underline{q}_j = \min\{q_i \mid i = j_0, j_0 + 1, \dots, j\} \quad (1.40)$$

$$\bar{q}_j = \max\{q_i \mid i = j_0, j_0 + 1, \dots, j\} \quad (1.41)$$

to provide checks on the behavior of the convergence. Note that the bounds are computed for $j \geq j_0$ to allow for initialization transients, for example with $j_0 = 2$. After J iterations, obtain the final estimate \hat{q}_J bounded below by \underline{q}_J and above by \bar{q}_J . The number of iterations J can be determined by a convergence criterion such as

$$|\hat{q}_j - \hat{q}_{j-1}| < \epsilon \quad (1.42)$$

for some absolute error tolerance ϵ or else J can be fixed by a predetermined value. This approach provides an iterative method by which to estimate the convergence order q without assuming its value *a priori* and without knowing the constant C .

Now let Δ^p be the finite difference operator [1, pg.255] of order p . Let $y^{(j)}[n]$ be the j^{th} iterative estimate at $t_n = nh_j$ of the function $y(t)$ for which we now assume the regularity $\rho = p + q$ with integer p and real q . Then we can use the method described above to estimate q in the sequence

$$e_j = \max_n |\Delta^p y^{(j)}[n]| / h_j^p \leq h_j^q \quad (1.43)$$

by testing iterates $y^{(j)}[n]$ with known p or an appropriate range of p . In fact, an effective automated algorithm can be implemented as an iterative search for p_k over $k = 1, 2, \dots$ where for each p_k a cycle of iterations over $j = 0, 1, 2, \dots, J_k$ is performed with the requirement that $J_k \geq 2$. Equation 1.42 provides a test of convergence of \hat{q}_j which determines J_k for a given cycle with p_k at iteration k . Now let

$$\rho_k = p_k + \hat{q}_{J_k} \quad (1.44)$$

denote the regularity estimate obtained with J_k iterations at finite difference order p_k . Values for p_{k+1} can be set from those for p_k by the recursion

$$p_{k+1} = \begin{cases} p_k + 1 & \text{if } \lceil \rho_k \rceil + 1 > p_k \\ p_k - 1 & \text{if } \lceil \rho_k \rceil + 1 < p_k \end{cases} \quad (1.45)$$

with initialization $p_1 = 2$ and termination if

$$\lceil \rho_k \rceil + 1 = p_k \quad (1.46)$$

or if k exceeds a predetermined maximum number of iterations. Then denote the final regularity estimate ρ_{Jp} where $J = J_k$ and $p = p_k$ from the final iteration k . Alternatively, both J and p can be fixed and predetermined. Finally, for an iterated $N \times M$ filter bank \mathbf{F} , compute the time domain regularity for each band filter as explained above using the function

$$\rho_{Jp} \equiv \lceil \rho_{mJp} \rceil = \text{tdr}(\mathbf{F}; J, p) \quad (1.47)$$

where the output parameter estimate $\boldsymbol{\rho}_{Jp}$ is a real M -vector.

Although this method does not insure monotonic convergence, it does provide faster convergence than the method described by Rioul [6, eqn.11.1]. Furthermore, both of Rioul's methods, the iterative estimate for the lower bound [6, eqn.11.1] and the noniterative estimate for the upper bound [6, eqn.13.1], require that the filter roots at $z = -1$ must be deconvolved prior to estimation of the filter's regularity. Thus, the iterative method presented here has the advantage that the roots at $z = -1$ do *not* need to be deconvolved prior to evaluation of the regularity estimate. As a consequence, it may be more appropriate in certain situations as an iterative estimate of the lower and upper bounds. However, when filter roots are available such as when filters are designed by spectral factorization, it is convenient to compute regularity estimates with Rioul's noniterative method for the upper bound. Therefore, $\rho = \text{tdr}(\mathcal{F})$ denotes estimates computed with Rioul's noniterative upper bound from the roots of $\mathcal{F}(z)$ (after deconvolving or otherwise excluding roots at $z = -1$), while $\boldsymbol{\rho}_{Jp} = \text{tdr}(\mathbf{F}; J, p)$ denotes estimates computed with Taswell's iterative estimate from the coefficients of \mathbf{F} . For examples with an experiment comparing these various estimates, refer to Table I of [14].

2.10. Frequency Domain Selectivity $\text{fds}(\mathbf{F})$

Define the frequency domain selectivity, denoted $\text{fds}(\mathbf{f})$ for the lowpass filter \mathbf{f} with frequency response $\mathcal{F}(\omega)$, with reference to an ideal M^{th} -band lowpass filter \mathbf{i} with response

$$\mathcal{I}(\omega) = \begin{cases} 1 & \text{if } \omega \in [0, \pi/M] \\ 0 & \text{if } \omega \in (\pi/M, \pi] \end{cases} \quad (1.48)$$

on the frequency interval $[0, \pi]$. Normalize the test filter \mathbf{f} with $\eta = 1 = \sum_n f[n]$ so that $\mathcal{F}(\omega) = 1$ at $\omega = 0$ (unit gain frequency response at DC). Let δ_1 and δ_2 be the passband and stopband magnitude deviation tolerances, respectively, with values such as $\delta_1 = \delta_2 = 1 \times 10^{-3}$.

Then define the passband edge ω_1 , stopband edge ω_2 , and transition bandwidth β with

$$\omega_1 = \min_{\omega|\chi=1} \omega \chi(|1 - |\mathcal{F}(\omega)|| > \delta_1) \quad (1.49)$$

$$\omega_2 = \max_{\omega|\chi=1} \omega \chi(|\mathcal{F}(\omega)| > \delta_2) \quad (1.50)$$

$$\beta = \omega_2 - \omega_1 \quad (1.51)$$

respectively. These parameters then permit definition of the frequency domain selectivity as the portion of the normalized passband interval

that correctly selects for the desired frequencies, that is, the ratio

$$(\pi/M - \beta)/(\pi/M) = 1 - \beta M/\pi. \quad (1.52)$$

However, such a definition does not adequately account for the magnitude of the deviation from ideal. Thus, define the area α of deviation from ideal as

$$\alpha = \int_0^\pi |\mathcal{I}(\omega) - |\mathcal{F}(\omega)|| d\omega \quad (1.53)$$

and the frequency domain selectivity as

$$\varsigma = \text{fds}(\mathbf{f}) = (\pi/M - \alpha)/(\pi/M) = 1 - \alpha M/\pi \quad (1.54)$$

which represents the portion of the normalized passband area of the magnitude frequency response that correctly selects for the desired frequencies.

Frequency domain selectivity for the M -band filter bank \mathbf{F} can be defined in a similar manner with reference to an ideal uniform M -band filter bank \mathbf{I} with lowpass \mathbf{i}_0 , bandpass $\{\mathbf{i}_m \mid m = 1, \dots, M - 2\}$, and highpass \mathbf{i}_{M-1} filters with ideal frequency responses

$$\mathcal{I}_0(\omega) = \begin{cases} 1 & \text{if } \omega \in [0, \pi/M] \\ 0 & \text{if } \omega \in (\pi/M, \pi] \end{cases} \quad (1.55)$$

$$\mathcal{I}_m(\omega) = \begin{cases} 0 & \text{if } \omega \in [0, m\pi/M) \\ 1 & \text{if } \omega \in [m\pi/M, (m+1)\pi/M] \\ 0 & \text{if } \omega \in ((m+1)\pi/M, \pi] \end{cases} \quad (1.56)$$

$$\mathcal{I}_{M-1}(\omega) = \begin{cases} 0 & \text{if } \omega \in [0, (M-1)\pi/M) \\ 1 & \text{if } \omega \in [(M-1)\pi/M, \pi] \end{cases} \quad (1.57)$$

for the frequency interval $[0, \pi]$. Then the area of deviation from the ideal for the m^{th} filter

$$\alpha_m = \int_0^\pi |\mathcal{I}_m(\omega) - |\mathcal{F}_m(\omega)|| d\omega \quad (1.58)$$

permits definition of the frequency domain selectivity as

$$\varsigma_m = \text{fds}(\mathbf{f}_m) = 1 - \alpha_m M/\pi \quad (1.59)$$

for the band filter \mathbf{f}_m , and as

$$\varsigma \equiv [\varsigma_m] = \text{fds}(\mathbf{F}) \quad (1.60)$$

for the filter bank \mathbf{F} . The integral in Equation 1.58 can be computed with simple numerical quadrature by trapezoidal rule as explained for the integrals in Section 2.8. Values for filters reported here represent numerical estimates based on the above definitions using magnitude frequency response. There exist analogous definitions using decibel frequency response.

2.11. Time Frequency Uncertainty $\text{tfu}(\mathbf{F})$

Discrete time frequency uncertainty, denoted $\text{tfu}(\mathbf{F})$ for the $N \times M$ filter bank \mathbf{F} , was computed with various modifications and extensions of the method of Haddad *et al.* [2, pg.1412] and reported as the areas of the Heisenberg uncertainty boxes with width σ_n and height σ_ω for each band filter \mathbf{f}_m in the filter bank. For the time domain energy, mean, and variance, compute

$$E_{n,m} = \sum_{n=0}^{N-1} |f_m[n]|^2 \quad (1.61)$$

$$\mu_{n,m} = E_{n,m}^{-1} \sum_{n=0}^{N-1} n |f_m[n]|^2 \quad (1.62)$$

$$\sigma_{n,m}^2 = E_{n,m}^{-1} \sum_{n=0}^{N-1} (n - \mu_{n,m})^2 |f_m[n]|^2 \quad (1.63)$$

for $m = 0, \dots, M - 1$. For the frequency domain with discrete Fourier transform $\mathcal{F}_m(\omega)$ of the band filter $f_m[n]$, it is necessary to determine the corresponding energy, mean, and variance values differently for the lowpass, bandpass, and highpass filters. For the energy, compute

$$E_{\omega,m} = \begin{cases} \int_{-\pi}^{\pi} |\mathcal{F}_m(\omega)|^2 d\omega & \text{if } 0 \leq m \leq M - 2 \\ \int_0^{2\pi} |\mathcal{F}_m(\omega)|^2 d\omega & \text{if } m = M - 1 \end{cases} \quad (1.64)$$

where the interval of integration differs only for the highpass filter. For the mean, compute

$$\mu_{\omega,m} = \begin{cases} E_{\omega,m}^{-1} \int_{-\pi}^{\pi} \omega |\mathcal{F}_m(\omega)|^2 d\omega & \text{if } m = 0 \\ E_{\omega,m}^{-1} \int_{-\pi}^{\pi} |\omega| |\mathcal{F}_m(\omega)|^2 d\omega & \text{if } 1 \leq m \leq M - 2 \\ E_{\omega,m}^{-1} \int_0^{2\pi} \omega |\mathcal{F}_m(\omega)|^2 d\omega & \text{if } m = M - 1 \end{cases} \quad (1.65)$$

where the integrand differs for the bandpass and the interval differs for the highpass. For the variance, compute

$$\sigma_{\omega,m}^2 = \begin{cases} E_{\omega,m}^{-1} \int_{-\pi}^{\pi} (\omega - \mu_{\omega,m})^2 |\mathcal{F}_m(\omega)|^2 d\omega & \text{if } m = 0 \\ E_{\omega,m}^{-1} \int_{-\pi}^{\pi} (|\omega| - \mu_{\omega,m})^2 |\mathcal{F}_m(\omega)|^2 d\omega & \text{if } 1 \leq m \leq M - 2 \\ E_{\omega,m}^{-1} \int_0^{2\pi} (\omega - \mu_{\omega,m})^2 |\mathcal{F}_m(\omega)|^2 d\omega & \text{if } m = M - 1 \end{cases} \quad (1.66)$$

where again the integrand differs for the bandpass and the interval differs for the highpass. Because the energy normalizations have been computed for each measure in its respective time or frequency domain, the above expressions should be valid regardless of the normalization constant used

by the discrete Fourier transform. Now determine the time frequency uncertainty

$$v_m = \sigma_{n,m} \sigma_{\omega,m} \quad (1.67)$$

as the product of the standard deviations in the time and frequency domains. For all discrete time filters, $v \geq 0.5$ with the optimal value 0.5 approached by binomial filters that tend to Gaussian functions in the limit [2]. Finally, let

$$\mathbf{v} \equiv [v_m] = \text{tfu}(\mathbf{F}) \quad (1.68)$$

denote the time frequency uncertainty for all filter bands in the filter bank. Note that the expressions introduced here apply to all bands of the filter bank including the highpass band omitted by Haddad *et al.* [2], and that these expressions differ from theirs with respect to the DFT-independent normalization used for all bands, as well as the integrands and intervals of integration used for the bandpass and highpass bands.

2.12. Conversion of M -Vector to Scalar Valued Parameters

Most of the evaluation test parameters presented here have been defined as $1 \times M$ vectors for $N \times M$ filter banks. Each element of the M -vector parameter provides information about the corresponding filter band in the filter banks. However, optimizations and/or comparisons are usually performed on scalars rather than vectors. As such, vector valued parameters can be readily converted to scalar valued parameters by computing a variety of statistics measuring central tendency such as the mean, weighted mean, or median, or those revealing extremes such as the minimum or maximum. With regard to extremes, it is often most appropriate to choose the extreme which corresponds to the worst case. For example, if the vector valued parameter is an error \mathbf{e} , then the corresponding scalar valued parameter is $e = \max_m e_m$. Analogously, for the delay \mathbf{d} and uncertainty \mathbf{v} , the worst case is the maximum, whereas for the regularity ρ and selectivity ς , it is the minimum.

2.13. Experiments with Test Evaluations of Filter Banks

Test evaluations were performed on filter banks with coefficients that were either generated from computational algorithms or obtained from published tables. Naming conventions established in [12] and further elaborated in [16, 18] for the filter banks there have been extended to apply to the various other filter banks tested here. Briefly, each 2-band family of filters has been named with an identifying acronym followed by

the parameters $(N_a, N_s; K_a, K_s)$ in the biorthogonal cases and by $(N; K)$ in the orthogonal cases where N is the number of filter coefficients, K is the number of filter roots at $z = -1$, and the subscripts \cdot_a and \cdot_s refer to the analysis and synthesis filter banks, respectively. The M -band families have been named with an acronym followed by the parameters $(N; M; K)$.

The families DRBBR, DCOMS, RROMS, and HRNSB were all generated from computational algorithms based on filter roots. The Daubechies Real Biorthogonal Balanced Regular DRBBR(10,10;5,5) and Daubechies Complex Orthogonal Most Symmetric DCOMS(22;11) filter banks were computed according to the method of Taswell [12, 16]. The Rioul Real Orthogonal Most Selective RROMS(20;2), RROMS(20;6), and RROMS(20;10) filter banks were computed in the following manner: i) Roots for the corresponding product filter were computed by Rioul's algorithm `remezwav` [8, pg:558]. ii) Roots for the minimum phase spectral factor were selected by choosing all the roots of the product filter inside the unit circle together with those roots on the unit circle at half their multiplicity. iii) These minimum phase spectral factor roots were then used to construct the coefficients for the RROMS(20; K) filter banks. Finally, the Hermite Real Nonorthogonal Symmetric Binomial HRNSB(5;5;4) filter bank was constructed from its roots according to the Z -transform definition of Haddad *et al.* [2, pg:1414].

The family SRORA was the only one generated from computational algorithms based on lattice angles. The Sherlock Real Orthogonal Random Angles SRORA(N ;2;1) filter banks were computed with both the original algorithm `orthogen` [9, p.1718] and the corrected algorithm [13] using $J = N/2$ random angles $\alpha_j \in [0, 2\pi)$, uniformly distributed and $(\pi/4)$ -sum normalized.

All other families were obtained from published tables listing filter coefficients. Those for the Heller Real Orthogonal M -band K -regular HROMK(8;4;2) filter bank were entered manually from the table in [3, pg:518]. Those for the various Nayebi-Barnwell-Smith filter banks were input from the tables in [5] by optical scanning and conversion to text characters with optical character recognition software. Coefficients published in [3] are tabulated in fixed precision to only four decimal places, whereas those in [5] are tabulated in full floating point precision with six digit mantissa and two digit exponent. Accuracy of the coefficients input was double-checked by painstaking comparison of the data between the printed page and computerized file displayed on monitor. This comparison was accomplished by two individuals with one person reading one format and the other person crosschecking the other format.

Both \mathbf{A} and \mathbf{S} were computed for the DRBBR filter banks which were the only biorthogonal filter banks tested. If only \mathbf{A} was computed or tabulated without \mathbf{S} for any of the other orthogonal or nonorthogonal filter banks, then \mathbf{S} defaulted to the paraconjugate of \mathbf{A} . All filter banks were η -normalized with $\eta = \sqrt{M}$ except for the HRNSB filter banks which were unit band energy normalized. Experimental evaluation test results reported here were computed with Version 4.5a2 of the `WVBOX` Software Library [10] running in Version 5.1.0 of the MATLAB technical computing environment [4] on a Toshiba Tecra 720CDT with the Windows 95 operating system.

3. Results

3.1. Tests on Filter Banks Generated by Computational Algorithms

Tables 1.1 and 1.2 present the parameter estimates for the DRBBR(10,10;5,5) and DCOMS(22;11) filter banks. Both of these examples demonstrate the performance of the evaluation tests on filter banks with coefficients generated to double precision by an algorithm for which there is a high degree of confidence regarding expected results [12, 16]. Both examples are minimum-length maximum-flatness 2-band Daubechies wavelet filter banks. For both, the experimentally observed delay d equals the theoretically expected value $N - 1$ where N is the length. Analogously, the empirical vanishing moments numbers ν equal the expected values $[0, K]$ where K is the number of lowpass filter zeros at $z = -1$. Both examples have reconstruction errors within the order of machine precision at $10^{-16} \leq e \leq 10^{-15}$. Additional errors for the biorthogonal example confirm presence of 2-shift biorthogonality with $e = 4.4 \times 10^{-16}$ but absence of 2-shift orthogonality with $e = 4.9 \times 10^{-1}$. The analogous errors for the orthogonal example confirm both 2-shift biorthogonality and orthogonality with $e = 2.4 \times 10^{-15}$.

Table 1.3 presents similar parameter estimates for the RROMS(20; K) filter banks for $K = 2, 6, 10$. These 2-band orthogonal wavelet filter banks [8] are related to the Daubechies collection [16] but do not have maximum flatness unless $K = N/2$, which is $K = 10$ for this sequence of examples with $N = 20$. Rioul and Duhamel [8] provided an algorithm `remezwav` only for the coefficients and roots of the nonorthogonal product filter, but did not provide nor demonstrate results of an algorithm for the orthogonal spectral factor filters that would be used for an orthogonal wavelet filter bank. Using the method for the orthogonal factors described in Section 2.13 with results as demonstrated in Table 1.3, there is a significant loss in orthogonality ranging from good orthogonal-

Table 1.1. DRBBR(10,10;5,5) Filter Bank Parameter Estimates.

Function	Band 0	Band 1
$\text{mrd}(\mathbf{A}, \mathbf{S})$	9	9
$\text{mre}(\mathbf{A}, \mathbf{S})$	3.89e-016	4.44e-016
$\text{mbe}(\mathbf{A}, \mathbf{S})$	4.44e-016	4.16e-016
$\text{moe}(\mathbf{A})$	4.86e-001	3.69e-001
$\text{fds}(\mathbf{A})$	0.4869	0.6338
$\text{fds}(\mathbf{S})$	0.6338	0.4869
$\text{tfu}(\mathbf{A})$	0.8883	0.5511
$\text{tfu}(\mathbf{S})$	0.5511	0.8883
$\text{tdr}(\mathbf{A}; J = 7, p = 3)$	1.2123	1.2077
$\text{tdr}(\mathbf{S}; J = 7, p = 4)$	2.3225	2.3203
$\text{tdm}(\mathbf{A}; J = 7, p = 3)$	1.41e-014	-1.96e-018
$\text{tdm}(\mathbf{S}; J = 7, p = 4)$	1.36e+000	2.61e-016
$\text{tdc}(\mathbf{A}; J = 7)$	4.4863	4.4863
$\text{tdc}(\mathbf{S}; J = 7)$	4.4863	4.4863
$\text{vmn}(\mathbf{A}; J = 7)$	0	5
$\text{vmn}(\mathbf{S}; J = 7)$	0	5

Table 1.2. DCOMS(22;11) Filter Bank Parameter Estimates.

Function	Band 0	Band 1
$\text{mrd}(\mathbf{A}, \mathbf{S})$	21	21
$\text{mre}(\mathbf{A}, \mathbf{S})$	2.89e-015	2.44e-015
$\text{mbe}(\mathbf{A}, \mathbf{S})$	2.44e-015	2.44e-015
$\text{moe}(\mathbf{A})$	2.44e-015	2.44e-015
$\text{fds}(\mathbf{A})$	0.8465	0.8465
$\text{tfu}(\mathbf{A})$	0.8357	0.8357
$\text{tdr}(\mathbf{A}; J = 6, p = 5)$	3.5658	3.5904
$\text{tdm}(\mathbf{A}; J = 6, p = 5)$	-1.29e-013	9.74e-015
$\text{tdc}(\mathbf{A}; J = 6)$	10.4258	10.4258
$\text{vmn}(\mathbf{A}; J = 6)$	0	11

Table 1.3. RROMS(20;K) Filter Bank Parameter Estimates.

Function	RROMS(20;2)		RROMS(20;6)		RROMS(20;10)	
	Band 0	Band 1	Band 0	Band 1	Band 0	Band 1
mrd(\mathbf{A}, \mathbf{S})	19	19	19	19	19	19
mre(\mathbf{A}, \mathbf{S})	9.47e-003	9.47e-003	3.34e-003	3.34e-003	9.01e-013	9.01e-013
moe(\mathbf{A})	9.47e-003	9.47e-003	3.34e-003	3.34e-003	9.01e-013	9.01e-013
fds(\mathbf{A})	0.8650	0.8650	0.8592	0.8592	0.8391	0.8391
tfu(\mathbf{A})	2.1513	2.1513	2.0113	2.0113	1.2777	1.2777
tdr($\mathbf{A}; J, p$)	0.4627	0.6201	1.5782	1.1722	3.4124	3.3431
tdm($\mathbf{A}; J, p$)	3.00e-001	2.10e+000	-3.07e-001	-4.95e-015	-4.85e-001	2.72e-014
tdc($\mathbf{A}; J$)	1.3779	9.5026	1.6979	9.4993	2.6665	9.4912
vmn($\mathbf{A}; J$)	0	2	0	6	0	10

$J = 6$ for all K while $p = 2, 3, 5$ for $K = 2, 6, 10$ respectively.

ity with negligible error at $e \approx 10^{-12}$ for $K = 10$ to poor orthogonality with significant error at $e \approx 10^{-2}$ at $K = 2$. The comparable reconstruction errors imply that perfect reconstruction can be achieved at $K = 10$ but not at $K = 2$ for $N = 20$. The stated motivation for the design of these filters was the increase of selectivity at the expense of regularity [8]. However, as measured by the selectivity ς , the increase is relatively insignificant from $\varsigma = 0.839$ to $\varsigma = 0.865$, while there is simultaneously a significant decrease in regularity from $\rho = 3.34$ to $\rho = 0.46$, and a significant increase in uncertainty from $v = 1.28$ to $v = 2.15$, as the zeros at $z = -1$ decrease from $K = 10$ to $K = 2$.

Table 1.4 presents the parameter estimates for HRNSB(5;5;4), a nonorthogonal filter bank with $N = M = 5$ and $K = 4$. This filter bank was constructed from symmetric binomials such that there are $K - m$ zeros at $z = -1$ and m zeros at $z = 1$ for bands $m = 0, 1, \dots, M - 1$ with an ideal value of 0.5 expected (in the limit as $K \rightarrow \infty$) for the time frequency uncertainty [2]. The empirical estimate $\mathbf{v} = [.503, .555, .513, .555, .502]$ confirmed this expectation. However, the frequency selectivity was poor with $\varsigma = -0.479$ and as expected, the filter bank was both nonreconstructing and nonorthogonal with significant reconstruction, biorthogonality, and orthogonality errors.

All of the preceding examples have demonstrated tests on filters generated with computational algorithms based on the filter polynomial roots. In contrast, Figure 1.1 displays results for an example that demonstrates tests on filters generated with computational algorithms based on the filter lattice angles. The M -shift orthogonality error $\text{moe}(\mathbf{F})$ is

Table 1.4. HRNSB(5;5;4) Filter Bank Parameter Estimates.

Function	Band 0	Band 1	Band 2	Band 3	Band 4
$\text{mrd}(\mathbf{A}, \mathbf{S})$	4	4	4	4	4
$\text{mre}(\mathbf{A}, \mathbf{S})$	6.05e-001	3.43e-001	6.95e-001	3.43e-001	6.05e-001
$\text{mbe}(\mathbf{A}, \mathbf{S})$	4.88e-002	0.00e+000	4.88e-002	0.00e+000	4.88e-002
$\text{moe}(\mathbf{A})$	4.88e-002	0.00e+000	4.88e-002	0.00e+000	4.88e-002
$\text{fds}(\mathbf{A})$	0.0013	-0.4616	-0.4793	-0.4616	0.0013
$\text{tfu}(\mathbf{A})$	0.5029	0.5550	0.5131	0.5550	0.5029
$\text{tdr}(\mathbf{A}; J = 3, p = 1)$	-0.3906	-0.3906	-0.3906	-0.3906	-0.3906
$\text{tdm}(\mathbf{A}; J = 3, p = 1)$	-8.73e-019	-2.65e-001	2.71e-018	-1.16e-018	-5.73e-018
$\text{tdc}(\mathbf{A}; J = 3)$	0.5008	0.5008	0.5008	0.5008	0.5008
$\text{vmn}(\mathbf{A}; J = 3)$	2	1	2	3	4

displayed as a function of the number of lattice angles $J = N/2$ for the SRORA($N;2;1$) filters computed with either the original algorithm (curve with ‘+’ markers) or the corrected algorithm (curve with ‘o’ markers). The original algorithm `orthogen` was not tested, and thus never validated, for $J \geq 4$ by the original authors [9]. The results displayed in Figure 1.1 demonstrate clearly that the original algorithm does *not* generate orthogonal wavelets for $J \geq 4$ whereas the corrected algorithm [13] resolves the problem. This problem was detected by using $\text{moe}(\mathbf{F})$ as an independent evaluation test for the experimental verification of the filter’s theoretical specifications.

3.2. Tests on Filter Banks Obtained from Published Tables

Table 1.5 presents parameter estimates for HROMK(8;4;2) which is an orthogonal M -band wavelet filter bank with $N = 8$, $M = 4$, and $K = 2$ zeros at $z = -1$ for the lowpass band filter. Despite the fixed precision of the filter bank coefficients to only four decimal places in the published tables [3], reconstruction, biorthogonality, and orthogonality were nevertheless confirmed with errors $e < 4 \times 10^{-5}$. However, selectivity was poor at $\varsigma = -0.216$ when compared with $\varsigma = 0.847$ for DCOMS(22;11), while uncertainty was good at $v = 0.928$ when compared with $v = 2.15$ for RROMS(20;2).

Table 1.6 presents a summary of test results for reconstruction error and delay for all filter banks tabulated in [5]. Despite the increased floating point precision with mantissa and exponent of these tabulated coefficients relative to the fixed precision of those tabulated in [3], only

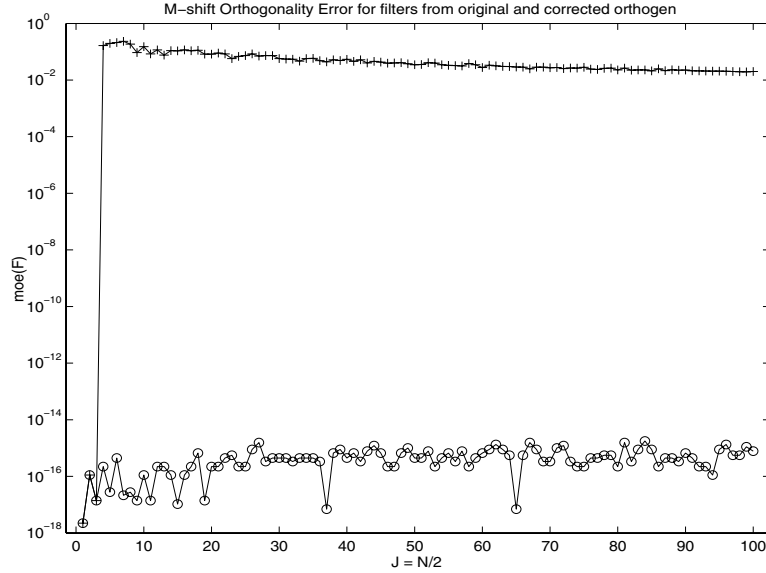


Figure 1.1. M -shift orthogonality error for filters from corrected and original orthogen.

Table 1.5. HROMK(8;4;2) Filter Bank Parameter Estimates.

Function	Band 0	Band 1	Band 2	Band 3
$\text{mrd}(\mathbf{A}, \mathbf{S})$	7	7	7	7
$\text{mre}(\mathbf{A}, \mathbf{S})$	2.91e-005	2.91e-005	3.01e-005	3.70e-005
$\text{mbe}(\mathbf{A}, \mathbf{S})$	3.63e-005	2.50e-005	2.50e-005	2.50e-005
$\text{moe}(\mathbf{A})$	3.63e-005	2.50e-005	2.50e-005	2.50e-005
$\text{fds}(\mathbf{A})$	0.4390	-0.2163	-0.2192	0.1440
$\text{tfu}(\mathbf{A})$	0.8462	0.9284	0.5505	0.5313
$\text{tdr}(\mathbf{A}; J = 4, p = 2)$	0.4450	0.4450	0.4450	0.4450
$\text{tdm}(\mathbf{A}; J = 4, p = 2)$	1.84e-002	-2.31e-001	6.25e-002	-1.64e-002
$\text{tdc}(\mathbf{A}; J = 4)$	0.7498	1.3372	0.5711	0.5928
$\text{vmn}(\mathbf{A}; J = 4)$	0	2	2	2

the example labeled “IV cosine modulated” achieved a comparable level of reconstruction with $e = 6 \times 10^{-5}$. There were four additional examples (II, V, VIII, and IX) that were approximately reconstructing with $10^{-4} \leq e \leq 10^{-3}$. However, there were two examples (III and VII) that

Table 1.6. Parameters for Coefficient Tables [5] of Nayebi-Barnwell-Smith Filter Banks.

Table	Description	Analytic Design			Numeric Estimate	
		N	M	Δ	$\text{mrd}(\mathbf{A}, \mathbf{S})$	$\text{mre}(\mathbf{A}, \mathbf{S})$
II	basic	55	5	54	54	1.08e-003
III	low delay	55	5	28	28	1.00e-001
IV	cosine modulated	55	5	54	54	6.13e-005
V	cosine modulated	96	16	95	95	1.08e-003
VII	linear phase	32	2	15	29	4.73e-001
VIII	low delay	32	2	15	15	1.25e-004
IX	low delay	32	2	7	7	2.98e-004

were not reconstructing with $e \geq 10^{-1}$. In one of these examples (VII), the observed delay $d = 29$ did not equal the design delay $\Delta = 15$.

4. Discussion

This report has presented detailed computational methods with validating experimental results for a comprehensive suite of evaluation tests that characterize the numerical properties of M -band filter banks represented as $N \times M$ matrices. By characterizing the numerical performance of analytic designs, these tests facilitate the experimental verification of theoretical specifications. All of the tests defined here are novel tests that apply to each of all bands of the filter banks. Thus, the tests return numerical estimates of a $1 \times M$ vector parameter in which the m^{th} element corresponds to the m^{th} column vector filter band of the $N \times M$ matrix filter bank. These M -vector valued estimates can be reduced to scalar valued estimates as explained in Section 2.12.

All of the empirical evaluation tests introduced here, including the Kronecker delta error (Section 2.3), M -shift biorthogonality error (Section 2.4), M -shift orthogonality error (Section 2.5), time domain centers and moments (Section 2.7), vanishing moments numbers (Section 2.8), time domain regularity (Section 2.9), and frequency domain selectivity (Section 2.10), have been devised independently by the author with the exception of the M -band reconstruction error (Section 2.6) and time frequency uncertainty (Section 2.11) which have been implemented as modifications and extensions of those in [5] and [2], respectively. These evaluation tests have been demonstrated and validated (Section 3) on a wide variety of filter banks with coefficients either generated by computational algorithms or obtained from published tables.

This work forms part of a major project to improve the scientific and engineering reproducibility of experiments with filter banks and transform algorithms by developing and using an evaluation methodology that addresses both specification and verification for each of three hierarchical stages consisting of filter bank coefficients, single-level convolutions, and multi-level transforms [11, 15]. Within the scope of this framework, this report has focused on the numerical verification of the filter bank coefficients. Complete verification of filter bank coefficients would benefit from both a comprehensive suite of numerical tests as well as graphical displays. An extensive set of multi-color visual plots for the filter bank examples demonstrated in this report can be viewed at the web site www.toolsmiths.com on the various pages devoted to the FirWav Filter Library. The plots viewable there include those corresponding to the numerical tests of this report as well as displays of the filter banks in the time domain, complex z domain, and frequency domain including magnitude, decibel, phase, unwrapped phase, phase delay, and group delay responses.

As often published in the literature, filter banks are characterized only by frequency domain plots of either magnitude or decibel response but not both. Nevertheless, failing to display both plots may hide important features not revealed by just one of the plots. Moreover, errors, whether reconstruction, orthogonality, or biorthogonality, are often not reported with numerical values. Yet it is difficult to make comparisons with only visual inspection of, for example, the magnitude frequency response plots. Thus, graphical displays (with the exception of Figure 1.1 which plots errors as a function of filter order) have been purposefully avoided in this report. Instead, attention has been directed at use of a comprehensive suite of numerical tests with values reported in tables. This approach readily facilitates explicit comparison of given filter banks.

While evaluation tests for estimating parameters may also be useful in optimizing filter bank designs [16], their primary use as demonstrated and advocated here focuses on the verification of coefficients rather than the generation of coefficients. Filter bank coefficients may be published in tables and then read and transcribed by people prior to use on computers rather than always being regenerated by computational algorithms. These coefficients may also be stored in data files, transmitted through communication channels, or perhaps even coded and decoded as part of a self-extracting data decompression system. Verification tests are thus necessary to detect errors that may arise at any step in any of these processes. Even if coefficients are always regenerated by a computational algorithm, the algorithm may be based on a certain method or design

parameter that may be completely unrelated to a different parameter of interest.

Therefore, a comprehensive suite of characterization and verification tests is necessary to evaluate the numerical performance of the filter coefficients on *all* relevant criteria. Moreover, in the general case of insuring reproducibility of filter algorithms and filter coefficients, *any* suite of tests that sufficiently characterizes and verifies the filter coefficients would suffice. However, in the specific case of making a claim about a certain filter characteristic, then the only test that is relevant is the test for that particular characteristic. For example, if a filter is claimed to be orthogonal, then the orthogonality test is the one that is relevant. Finally, empirical tests can be used to evaluate for equivalent performance of filter families with respect to certain characteristics within given tolerances [18, 19].

Tables 1.1, 1.2, 1.5, and 1.4 demonstrated respectively examples of real biorthogonal 2-band, complex orthogonal 2-band, real orthogonal 4-band, and real nonorthogonal 5-band filter banks for which observed values were consistent with expected values for parameters. These examples, and many others in [14, 16, 18] and elsewhere, serve to validate the evaluation tests. However, Tables 1.6 and 1.3 and Figure 1.1 all demonstrated examples with significant discrepancies between analytical design and experimental evaluation parameters. With regard to the discrepancies in the results for Table 1.6 which involved filter banks with tabulated coefficients published in [5], one of the authors, M. J. T. Smith, suggested¹ that the most likely source of the problem could be “flipped signs” incurred when the original manuscript was typeset by the printer. With regard to the discrepancies in the results for Table 1.3 which involved filter banks with computed coefficients, it is possible that the loss of orthogonality could be attributed to numerical instabilities in the computation of the double roots on the unit circle output by the function `remezwav`. This instability impacted the orthogonal spectral factor filters but not the nonorthogonal product filter. Finally, with regard to the discrepancies depicted in Figure 1.1, it is apparent as established by the corrected algorithm [13] that the original algorithm `orthogen` was not consistent with the original authors’ mathematical and diagrammatical specification [9].

These three sets of examples with discrepancies demonstrate situations where the empirical evaluation tests detected what can be called *transmission*, *interpretation*, and *implementation* errors, respectively. Notably in the second and third cases in contrast to the first case, the errors appeared in the published literature, not because of an alleged transmission (typographical or communication) error, but because of a

failure to require, perform, and report any independent evaluation tests with conclusions based on empirical results. Instead, conclusions were merely assumed to be true based on theoretical expectations (analytic design and algorithm specification) without experimental observation and verification. For example, if Sherlock and Monro [9] had performed independent tests of orthogonality for all J including $J \geq 4$, it is probable that they would have detected the implementation error in their algorithm `orthogen`. Analogously, if Rioul and Duhamel [8] had computed the orthogonal spectral factors and numerically evaluated their orthogonality, it is probable that they would have detected the interpretation error for their algorithm `remezwav`. As a consequence, they probably would not have used the term *orthogonal* in the title of their paper. Alternatively, they could have offered the following discussion of the *pseudo-orthogonality* of their filter banks.

It remains unclear whether orthogonal spectral factors can be computed in a numerically stable manner with the algorithm `remezwav`, or whether the roots output by `remezwav` can be sufficiently refined by a subsequent root polishing algorithm prior to the spectral factorization. An opposing interpretation would be to consider the filter banks *orthogonal* or *pseudo-orthogonal* even though the error deteriorates, for the example in Table 1.3, from negligible at 10^{-12} for RROMS(20;10) to significant at 10^{-2} for the RROMS(20;2). However, recall that the RROMS(20;10) is equivalent to a Daubechies minimum-length maximum-flatness filter bank and that the claimed advantages of the RROMS(20;2) in terms of increased selectivity do not appear to be significant enough to compensate for the loss of orthogonality, regularity, uncertainty, *et c.*, as demonstrated in Table 1.3. In any event, the trade-offs involved should be explicitly noted in any discussion of the filter banks' advantages and disadvantages.

The various descriptive terms such as *significant*, *moderate*, and *negligible* have been used here in a relative sense. Thus, they depend on the context of the problem and the judgement of the investigator. Generally, as used here, the terms *significant* and *nonreconstructing* have been loosely applied to errors $e \geq 10^{-2}$, *moderate* and *approximate reconstructing* to errors $10^{-2} \geq e \geq 10^{-4}$, *minimal* and *near-perfect reconstructing* to errors $10^{-5} \geq e \geq 10^{-10}$, and finally *negligible* and *perfect reconstructing* to errors $e \leq 10^{-10}$. These rankings are based on the assumption that the order of machine precision corresponds to $10^{-16} \leq e \leq 10^{-15}$. Additional examples validating and demonstrating the filter bank evaluation tests elaborated here can be found in [14, 16, 18]. However, the brief survey of examples that have been analyzed and reported here has demonstrated that papers in the published

literature contain errors of transmission, implementation, and interpretation. These errors were not detected by the original authors, referees, and editors. It is unlikely that additional errors, whether past or future, will be detected and/or prevented without the use of independent evaluation tests which require that as much attention and importance be accorded to experiment as to theory.

A fundamental tenet of investigative science and engineering requires that conclusions must be based on methods and results that are reproducible and valid. The general notions of experimental validity and reproducibility can be said in one sense to correspond, respectively, to the specific notions of accuracy (bias) and precision (variance). To improve the validity and reproducibility of filter bank investigations, empirical tests for the evaluation of filter banks should be required for the characterization and verification of the numerical performance of filter bank coefficients. Such an evaluation enables the comparison of filter banks and optimization of their designs, but more importantly, facilitates the detection and prevention of errors and discrepancies in the computed or tabulated coefficients and the generating algorithms for those coefficients. Automated detection of errors and discrepancies with appropriate experimental evaluation methodologies becomes increasingly important in an era of increased pressure on the peer review process with the accompanying increased numbers of mistakes appearing in the published literature. As a consequence, these empirical tests will insure greater reproducibility and validity of results and the conclusions based on those results. The importance of an evaluation methodology, with both a specification and a verification component, can be neither ignored nor trivialized.

Acknowledgments

Filter banks from [5] were evaluated in an extensive test of tabulated coefficients available from a data file (in contrast to computed coefficients obtained by executing an algorithm). Electronic data files were not available from the original authors. I thank J.N. for graciously assisting me with entering and double-checking these tables of coefficients.

Notes

1. M. J. T. Smith, personal communication, February 1998.

References

- [1] Germund Dahlquist and Ake Bjorck. *Numerical Methods*. Prentice-Hall, Inc., Englewood Cliffs, NJ, 1974.
- [2] Richard A. Haddad, Ali N. Akansu, and Adil Benyassine. Time-frequency localization in transforms, subbands, and wavelets: A critical review. *Optical Engineering*, 32(7):1411–1429, 1993.
- [3] Peter Niels Heller. Rank m wavelets with n vanishing moments. *SIAM Journal on Matrix Analysis and Applications*, 16(2):502–519, April 1995.
- [4] The MathWorks, Inc., Natick, MA. *MATLAB The Language of Technical Computing: MATLAB 5.1 New Features*, May 1997.
- [5] Kambiz Nayebi, Thomas P. Barnwell III, and Mark J. T. Smith. Time-domain filter bank analysis: A new design theory. *IEEE Transactions on Signal Processing*, 40(6):1412–1429, June 1992.
- [6] Olivier Rioul. Simple regularity criteria for subdivision schemes. *SIAM Journal on Mathematical Analysis*, 23(6):1544–1576, November 1992.
- [7] Olivier Rioul. A discrete-time multiresolution theory. *IEEE Transactions on Signal Processing*, 41(8):2591–2606, August 1993.
- [8] Olivier Rioul and Pierre Duhamel. A Remez exchange algorithm for orthonormal wavelets. *IEEE Transactions on Circuits and Systems II. Analog and Digital Signal Processing*, 41(8):550–560, August 1994.
- [9] B. G. Sherlock and D. M. Monro. On the space of orthonormal wavelets. *IEEE Transactions on Signal Processing*, 46(6):1716–1720, June 1998.
- [10] Carl Taswell. *WAVBOX Software Library and Reference Manual*. Computational Toolsmiths, www.wavbox.com, 1993–2000.
- [11] Carl Taswell. Specifications and standards for reproducibility of wavelet transforms. In *Proceedings of the International Conference on Signal Processing Applications and Technology*, pages 1923–1927. Miller Freeman, October 1996.
- [12] Carl Taswell. Computational algorithms for Daubechies least-asymmetric, symmetric, and most-symmetric wavelets. In *Proceedings of the International Conference on Signal Processing Applications and Technology*, pages 1834–1838. Miller Freeman, September 1997.
- [13] Carl Taswell. Correction for the Sherlock-Monro algorithm for generating the space of real orthonormal wavelets. Technical Report CT-1998-05, Computational Toolsmiths, www.toolsmiths.com, June 1998.

- [14] Carl Taswell. Numerical evaluation of time-domain moments and regularity of multirate filter banks. In *Proceedings of the IEEE Digital Signal Processing Workshop*, volume 1, August 1998. Paper #71.
- [15] Carl Taswell. Reproducibility standards for wavelet transform algorithms. Technical Report CT-1998-01, Computational Toolsmiths, www.toolsmiths.com, March 1998.
- [16] Carl Taswell. A spectral-factorization combinatorial-search algorithm unifying the systematized collection of Daubechies wavelets. In V. B. Bajić, editor, *Proceedings of the IAAMSAD International Conference SSCC'98: Advances in Systems, Signals, Control, and Computers*, volume 1, pages 76–80, September 1998. Invited Paper and Session Keynote Lecture.
- [17] Carl Taswell. The systematized collection of Daubechies wavelets. Technical Report CT-1998-06, Computational Toolsmiths, www.toolsmiths.com, June 1998.
- [18] Carl Taswell. Least and most disjoint root sets for Daubechies wavelets. In *Proceedings of the IEEE International Conference on Acoustics, Speech, and Signal Processing*, 1999. Paper #1164.
- [19] Carl Taswell. Constraint-selected and search-optimized families of Daubechies wavelet filters computable by spectral factorization. *Journal of Computational and Applied Mathematics*, 121:179–195, 2000. Invited Paper, Special Issue on Numerical Analysis in the Twentieth Century.